

NLO PREDICTION FOR THE PHOTOPRODUCTION
OF THE ISOLATED PHOTON AT HERA

Maria Krawczyk* and Andrzej Zembrzusi

Institute of Theoretical Physics, Warsaw University,
ul. Hoża 69, 00-681 Warsaw, Poland
E-mail: krawczyk@fuw.edu.pl, azem@fuw.edu.pl**Abstract**

The NLO calculation of the DIC process with the isolated photon is presented and the comparison is made with the other NLO calculation and with recent measurement at HERA. The satisfactory agreement was found.

* Talk at ICHEP'98, Vancouver, Canada, 23-29 July 1998

NLO PREDICTION FOR THE PHOTOPRODUCTION OF THE ISOLATED PHOTON AT HERA

M. KRAWCZYK, A. ZEMBRZUSKI

Institute of Theoretical Physics, Warsaw University, ul. Hoża 69, 00-681 Warsaw, Poland

E-mail: krawczyk@fuw.edu.pl, azem@fuw.edu.pl

The NLO calculation of the DIC process with the isolated photon is presented and the comparison is made with the other NLO calculation and with recent measurement at HERA. The satisfactory agreement was found.

1 Introduction

We consider Deep Inelastic Compton (DIC) scattering where the photon with large transverse momentum p_T is produced in ep collision. With antitagging or untagging conditions such reaction is dominated by events with almost real photons mediating the ep interaction, $Q^2 \approx 0$, so in practice the photoproduction is considered. The observed final γ arises directly from the direct subprocess $\gamma q \rightarrow \gamma q$ or from subprocesses where partonic content of the photon contributes. The final photon may originate also from the fragmentation processes, where q or g 'decays' into γ .

In this talk the results of the NLO calculation for DIC process¹ are shown with the discussion on the choice of the relevant set of diagrams. Then the influence of the isolation cuts on the production rate of the final photon is shown and the role of additional cuts applied in the experimental analysis of this process at HERA is discussed. The importance of the box diagram $\gamma g \rightarrow \gamma g$, being the higher order direct process, is stressed.

The final results for the isolated photon production in the DIC process at HERA are compared with the existing in literature calculation² and with the corresponding data³.

2 Deep inelastic Compton process in NLO

2.1 NLO calculation for processes involving photons

We start by describing processes which are (should be?) included in the NLO QCD calculation of the cross section for the DIC process,

$$\gamma p \rightarrow \gamma X. \quad (1)$$

Although we will discuss the process (1), the problem which we touch upon is more general - it is related to the different approaches to NLO calculations of cross sections for hadronic processes involving photons.

The Born level contribution to the cross section, the lowest order in the strong coupling constant α_s term, is based on the Compton process on the quark (Fig. 1):

$$\gamma q \rightarrow \gamma q. \quad (2)$$

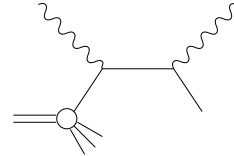


Figure 1: The lowest order Born contribution

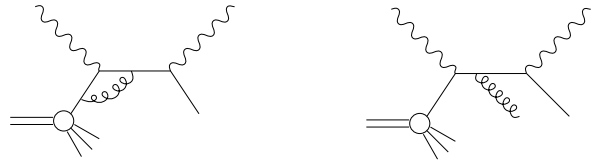


Figure 2: Examples of the virtual and real α_s corrections to the Born contribution

It leads to the $[\alpha_{em}^2]$ order contributions to the partonic cross section, and at the same α_{em}^2 order it contributes to the hadronic cross section for the process $\gamma p \rightarrow \gamma X$. In the NLO analysis the α_s corrections to (2) are calculated and the terms of order $\alpha_{em}^2 \alpha_s$ appear (Fig. 2).

The Parton Model prediction for the DIC process, which applies for $x_T = 2p_T/\sqrt{S} \sim \mathcal{O}(1)$, relies solely on the Born contribution (2)⁴. For semihard processes, where $x_T \ll 1$, the prediction based on (2) is not a good approximation, since now one should consider besides (2) also contributions involving interactions of the partonic content of the photon(s). There are two classes of such contributions: single resolved with resolved initial or final photon, and double resolved with both the initial and the final photon resolved (Figs. 3, 4). They give contributions to partonic cross sections of orders $[\alpha_{em}\alpha_s]$ (single resolved) and $[\alpha_s^2]$ (double resolved). If one takes into account that partonic densities in the photon and the parton fragmentation into the photon are of order $\sim \alpha_{em}$, the final contribution to the hadronic cross section from resolved photon processes are $\sim \alpha_{em}^2 \alpha_s$ and $\alpha_{em}^2 \alpha_s^2$, respectively. In the LLO approach these three types of subprocesses: with two direct photons, with one and two resolved photons, convoluted with the relevant LL parton densities, are considered⁵.

In the NLO approach, among $\alpha_{em}^2 \alpha_s$ terms, there are

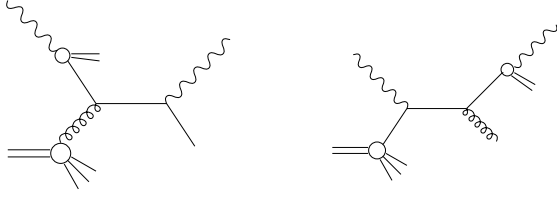


Figure 3: Examples of single resolved processes. a) the resolved initial photon, b) the resolved final photon

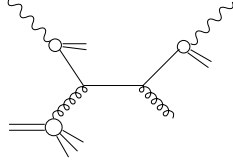


Figure 4: An example of double resolved photon process

terms related to the collinear singularities, which then have to be subtracted and treated as a part of the corresponding single resolved photon contribution. At the same time in the NLO expression there are no collinear singularities terms which would correspond to the double resolved photon contributions. It indicates that taking into account subprocesses $[\alpha_s^2]$ associated with the both initial and final photons resolved goes beyond the accuracy of the NLO calculation. This will be consistent within the NNLO approach, where α_s^2 correction to the Born term and α_s correction to the single resolved terms should be included, all giving the same $\alpha_{em}^2 \alpha_s^2$ order contribution to the hadronic cross sections.

The other set of diagrams is considered by some authors in the NLO approach to DIC process (1), due to their different way of the counting the order of the parton densities in the photon (or the parton fragmentation into the photon)⁶. This approach, which we will call “ $\frac{1}{\alpha_s}$ ” approach to the structure of photon, is motivated by the existence of the large logarithms of Q^2 in the F_2^γ already in PM. By expressing $\ln(Q^2/\Lambda_{QCD}^2)$ as $\sim \frac{1}{\alpha_s}$ one treats the parton densities in photon as proportional to α_{em}/α_s . By applying this method to the DIC process, we see that here the single resolved photon contribution to the hadronic cross section is of the same order as the Born term, namely

$$\frac{\alpha_{em}}{\alpha_s} \otimes [\alpha_{em} \alpha_s] \otimes 1 = \alpha_{em}^2, \quad (3)$$

also the double resolved photon contribution is of the same order

$$\frac{\alpha_{em}}{\alpha_s} \otimes [\alpha_s^2] \otimes \frac{\alpha_{em}}{\alpha_s} = \alpha_{em}^2. \quad (4)$$

We see that this way, the same α_{em}^2 order contributions

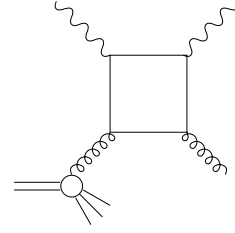


Figure 5: The box diagram

to the hadronic cross section are given by the Born direct process, single resolved photon and double resolved photon processes, although they correspond to quite different final states (observe a lack of the remnant of the photon in the direct process). Moreover, they constitute the lowest order (in the strong coupling constant) term in the perturbative expansion, actually the zeroth order, so the (leading) dependence on the strong coupling constant is absent. If one takes into account that some of these terms correspond to the hard processes involving gluons, a lack of α_s coupling in the cross section seems to be contrary to the intuition. On the other hand, on such set of contributions the LL prediction is based.

In this approach beside the α_s correction to the Born process also the α_s corrections to the single and to the double resolved photon processes should be included in the NLO calculation, since all of them give terms of the same order, $\alpha_{em}^2 \alpha_s$.

To summarize, the first NLO approach starts with one basic, direct subprocess, while the second one with three different subprocesses (as in LO). Obviously, some of NNLO terms in the first method belong to the NLO terms in the second one.

2.2 α_{em}^2 , $\alpha_{em} \alpha_s$ and α_s^2 subprocesses in DIC

Below we will discuss our NLO analysis of the DIC process¹, where the parton densities in the photon (the parton fragmentation into the photon) are treated as $\sim \alpha_{em}$.

In the NLO calculation of the DIC process we take the following subprocesses into account:

- the Born contribution (2) (Fig. 1)
- the α_s corrections to the Born diagram (Figs. 2)
- two types of single resolved photon contributions, with the resolved initial and with the resolved final photon (Figs. 3)

Beside the above set of diagrams, the full NLO set, we will in addition include two terms of order $\alpha_{em}^2 \alpha_s^2$ (formally from the NNLO set): the double resolved contributions (Fig. 4) and the direct box diagram $\gamma g \rightarrow \gamma g$ (Fig. 5), since they were found to be large⁷.

2.3 Inclusive cross section for the DIC process at ep colliders

Infrared singularities which appear in the NLO calculations of the virtual corrections to the Born process are canceled by infrared singularities in the real corrections. All collinear (mass) singularities are factorized into structure and fragmentation functions, as discussed above, leading to the final formula for the inclusive cross section for the $\gamma p \rightarrow \gamma X$ scattering:

$$E_\gamma \frac{d^3\sigma^{\gamma p \rightarrow \gamma X}}{d^3p_\gamma} = \sum \int \frac{dz}{z^2} \int dx_\gamma \int dx f_{a/\gamma}(x_\gamma, \bar{Q}^2) f_{b/p}(x, \bar{Q}^2) \cdot D_{\gamma/c}(z, \bar{Q}^2) E_\gamma \frac{d^3\sigma^{ab \rightarrow cd}}{d^3p_\gamma} + \sum \int dx f_{b/p}(x, \bar{Q}^2) \frac{\alpha_S}{2\pi^2 \hat{s}} K_b, \quad (5)$$

where the second term, K-term, describes the QCD corrections to the Born process and the first term is a sum over all the other contributions. The $f_{b/p}$ is a b parton distribution in the proton while $f_{a/\gamma}$ is a a parton distribution in the photon. For direct initial photon (where $a = \gamma$): $f_{a/\gamma} = \delta(x_\gamma - 1)$. $D_{\gamma/c}$ is a c parton fragmentation function into a photon, or for non-fragmentation processes (where $c = \gamma$) $D_{\gamma/c} = \delta(z - 1)$. x , x_γ , z are: a part of the initial proton momentum taken by the b parton, a part of the initial photon momentum taken by the a parton, and a part of the c parton momentum taken by the final photon, respectively. The \bar{Q} scale is provided here by the p_T .

Denoting the differential cross section for the γp scattering (1) by $\tilde{\sigma}^{\gamma p}$ we now relate it to the corresponding ep cross section. The differential cross section for the ep scattering in the antitagging conditions can be calculated using the equivalent photon approximation:

$$\tilde{\sigma}^{ep} = \int G_{\gamma/e}(y) \tilde{\sigma}^{\gamma p} dy, \quad (6)$$

where $y = E_\gamma/E_e$ is a fraction of the initial electron energy taken by the photon, and the (real) photon distribution in the electron is given by:

$$G_{\gamma/e}(y) = \frac{\alpha}{2\pi} \cdot \left\{ \frac{1 + (1-y)^2}{y} \ln \left[\frac{Q_{max}^2(1-y)}{m_e^2 y^2} \right] - 2(1-y) + \frac{2m_e^2 y^2}{Q_{max}^2} \right\}, \quad (7)$$

with m_e being the electron mass. The Q_{max}^2 value we assume as equal to 1 GeV², which is typical for the photoproduction measurements at HERA collider.

2.4 Isolated photon production in DIC process

In order to reduce backgrounds from π^0 's and γ 's radiated from final state hadrons isolation cuts on the observed photon have to be performed. Experimentally the

isolation cuts are defined by demanding that a sum of hadronic energy within a cone of radius R around the final photon should be smaller than the final photon energy multiplied by parameter $\epsilon \sim 0.1$:

$$\sum_{hadrons} E_h < \epsilon E_\gamma. \quad (8)$$

The radius is defined in the rapidity and azimuthal angle phase space: $R = \sqrt{\Delta\Phi^2 + \Delta\eta^2}$.

The simplest way to calculate the differential cross section for isolated photon, $\tilde{\sigma}^{isol}$, is to calculate difference of an inclusive differential cross section, $\tilde{\sigma}^{incl}$, and a subtraction term, $\tilde{\sigma}^{subt}$ (see⁸):

$$\tilde{\sigma}^{isol} = \tilde{\sigma}^{incl} - \tilde{\sigma}^{subt}. \quad (9)$$

By the subtraction term we mean differential cross section with cuts opposite to the isolation cuts, i.e. within a cone of radius R around the final photon there should appear hadrons with total energy higher than the photon energy multiplied by ϵ :

$$\sum_{hadrons} E_h > \epsilon E_\gamma. \quad (10)$$

The cuts are imposed in the partonic phase space integration (for K-term) and integration over z (for fragmentation processes).

We calculate the subtraction term in an approximate way, with two simplifying assumptions⁹:

- the parameter ϵ is small, $\epsilon \ll 1$
- an angle δ between the final photon and a parton (from which a hadronic jet arise) inside the cone is small (i.e. the cone is small) and can be approximated by $\delta = R/\cosh(\eta)$, where η is the rapidity of the photon.

The above approximations are used only when calculating the K-term (i.e. the QCD corrections to the Born process) in the subtraction term $\tilde{\sigma}^{subt}$. Because this term gives about 4% of the inclusive cross section, we expect that the error resulting from using the approximations is negligible.

3 Results

3.1 Inclusive cross section

First we will discuss the general features of the inclusive cross section for the DIC process in the ep collision. We take the HERA collider energies: $E_e=27.5$ GeV, $E_p=820$ GeV and we limit ourselves to the p_T range of the final photon between 5 and 10 GeV (x_T is 0.03-0.07). The calculation was performed in $\overline{\text{MS}}$ scheme and as a hard (renormalization, factorization) scale we take $\bar{Q} = p_T$, also $\bar{Q} = p_T/2$ and $2p_T$ was studied. Number of active flavours is assumed to be $N_f=4$ (and for comparison

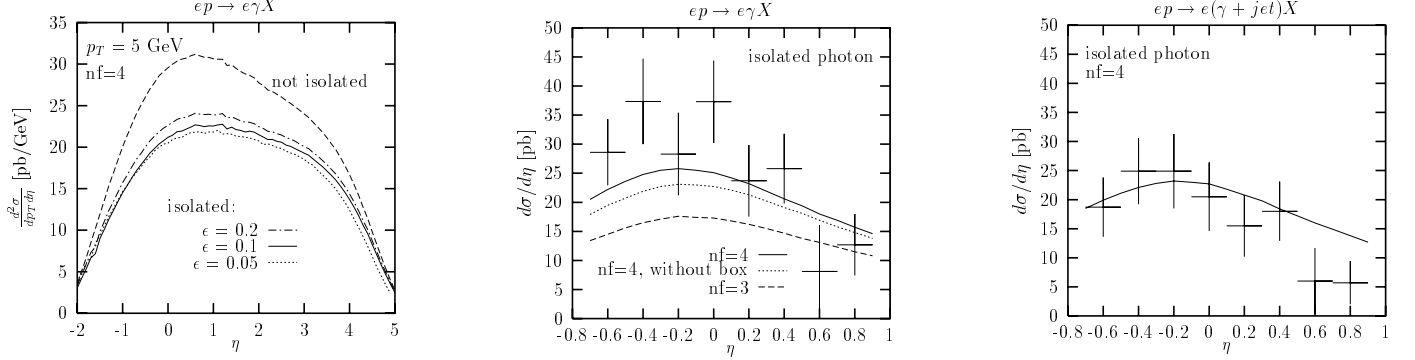


Figure 6: The photon rapidity distributions. a) The differential cross section $d^2\sigma/dp_T d\eta$ integrated over whole range of y for $p_T=5$ GeV for the final photon not isolated (upper line) or isolated with $R=1$ and $\epsilon=0.05, 0.1, 0.2$. b) The cross section $d\sigma/d\eta$ integrated over $0.16 \leq y \leq 0.8$ and $5 \text{ GeV} \leq p_T \leq 10 \text{ GeV}$ for the isolated final photon with $R=1$ and $\epsilon=0.1$. The result for $N_f=4$ (solid line) and for comparison the same without the box contribution (dotted line). The result for $N_f=3$ (dashed line) is also shown. c) The cross section as in b) for $N_f=4$ for the isolated photon plus jet production, where the jet obeys conditions: $-1.5 \leq \eta^{jet} \leq 1.8$ and $p_T^{jet} \geq 5 \text{ GeV}$ (solid line). The data are the ZEUS experiment preliminary results³.

$N_f=3$). N_f enters into the evaluation of the coupling constant α_s . Note that the assumed NLO form of α_s plays a role, as changing the form from:

$$\alpha_s = \frac{4\pi}{\beta_0 \ln(\bar{Q}^2/\Lambda_{QCD}^2)} \frac{1}{1 + \frac{2\beta_1}{\beta_0^2} \frac{\ln[\ln(\bar{Q}^2/\Lambda_{QCD}^2)]}{\ln(\bar{Q}^2/\Lambda_{QCD}^2)}} \quad (11)$$

to

$$\alpha_s = \frac{4\pi}{\beta_0 \ln(\bar{Q}^2/\Lambda_{QCD}^2)} \left[1 - \frac{2\beta_1}{\beta_0^2} \frac{\ln[\ln(\bar{Q}^2/\Lambda_{QCD}^2)]}{\ln(\bar{Q}^2/\Lambda_{QCD}^2)} \right] \quad (12)$$

($\beta_0 = 11 - 2/3N_f$ and $\beta_1 = 51 - 19/3N_f$) changes the results by 5%. The final results will be given using the latter form with parameters: $\Lambda_{QCD}=0.2 \text{ GeV}$ for $N_f=4$ and 0.248 GeV for $N_f=3$.

We use Glück, Reya, Vogt NLO parametrizations of the proton structure function, the photon structure function and the fragmentation function¹⁰, for comparison also other photon structure functions are used^{11,12}. The value Λ_{QCD} was used here as fitted to the data.

The importance of the particular contributions to the cross section can be illustrated by the following results obtained for the *inclusive* cross section integrated over $5 \text{ GeV} < p_T < 10 \text{ GeV}$ (where the sum over all subprocesses is equal to 210 pb): *Born* = 41.2%, *single resolved* = 34.2%, *double resolved* = 15.7%, *box* = 5.4%, *K-term*=3.9%. So it is obvious that the single resolved photon processes give contribution comparable to the Born term. Also the double resolved photon processes are important giving half of the single resolved photon process contribution. The overall double resolved photon cross section is build from many, relatively small, individual terms. The box diagram gives 14% of the Born contribution- relatively large box contribution is due to large gluonic content of the proton at small x_p (the Born process bases on the quark density at the same value x_p).

3.2 Inclusive versus isolated photon cross section

The isolation cut was introduced with the radius $R = 1$, and $\epsilon=0.05, 0.1$ and 0.2 . Results are presented in Fig.6a where the *inclusive* cross section and the *isolated* photon cross sections are compared. Large effect is seen when the isolation cut is imposed on the final photon in DIC process, with a larger suppression of the fragmentation processes (up to 80%, see⁹) as expected. This effect is not very sensitive to the value of ϵ .

3.3 Comparison with data

To compare our results with data the calculations were performed for the HERA collider energies with cuts used in the ZEUS experiment³. For the isolated photon production in DIC process we take $R=1$, $\epsilon=0.1$ and consider ranges: $5 \text{ GeV} \leq p_T \leq 10 \text{ GeV}$, $0.16 \leq y \leq 0.8$. Two types of final state were measured:

" γ " – an isolated photon with rapidity $-0.7 \leq \eta^\gamma \leq 0.9$, " γ +jet" – the isolated photon as above plus the jet with $-1.5 \leq \eta^{jet} \leq 1.8$, $p_T^{jet} \geq 5 \text{ GeV}$.

In Fig.6b the isolated photon rapidity distributions with the above criteria are shown. The importance of the box diagram is seen (the double resolved contribution is smaller than box up to factor 2 for negative η^γ). Note also a large difference between results for $N_f=4$ and 3 (due to fourth power of electric charge characterizing processes involving two photons). The prediction based on the four massless quarks overestimates the production rate, while this with $N_f=3$ underestimates this rate. We believe that the true prediction lies between two curves, but closer to the upper one. (The proper treatment of the charm quark is crucial here and will be discussed elsewhere¹³). In Fig.6c the results for the final state with a photon and the jet are presented. The calculation bases

Table 1: DIC cross section (pb) for $0.8 \leq x_\gamma \leq 1$

<i>subprocess</i>	<i>tot</i>	<i>Born</i>	<i>box</i>	<i>2res</i>
γ	25.2	16.3	3.2	0.39
$\gamma + jet$	23.4	15.1	3.0	0.27

here on the additional assumption and therefore should be treated as an estimation of the considered cross section (see⁹ for details). Reasonable agreement with data are found for both final states (Figs.6b,c).

Below we discuss results for the isolated photon cross sections within the ZEUS cuts listed above, and integrated over $0.8 \leq x_\gamma \leq 1$ – a “direct” sample. Particular contributions to the isolated photon cross section are presented in Table 1 for “ γ ” and “ $\gamma+jet$ ” in the final state. (Results correspond to $N_f=4$). The total contribution for “ $\gamma+jet$ ” is smaller by 2 pb as compared to “ γ ”, nevertheless the following ratios have similar pattern in both cases: “Born/tot”=65% and “box/tot”=13%. We see how much the role of the direct processes is enhanced by the isolation cut and the range of η^γ . Note also that now “box/Born”=20%, while the “2res/Born” \sim 2%.

Results obtained using other choices of the scale \bar{Q} : $\bar{Q}=p_T/2$, $2p_T$, differ from ones based on the reference scale p_T by $\pm 4\%$ (6%) for “ γ ” (“ $\gamma+jet$ ”) final state. The results based on ACFGP or GS parton parametrization for the photon differ from GRV predictions by less than 4%.

The ZEUS measurement for the “ $\gamma+jet$ ” final state leads to cross section equals to $15.4 \pm 1.6 \pm 2.2 \text{ pb}^3$.

3.4 Comparison with other results

Our NLO calculation of DIC process differs from NLO analysis presented in Ref.[2], based on the “ $1/\alpha_s$ ” approach, by types of subprocesses included. In our analysis we do not include α_s corrections to the single resolved processes, the NNLO term. On the other hand we include the box diagram, although being also beyond the NLO accuracy, it was found to be large especially in the experimental conditions used in the ZEUS experiment. Our prediction (GRV parton parametrizations with $N_f = 4$, scale $\bar{Q}=p_T$) for the rapidity distribution for the “ γ ” is lower by 10% to 25% for the negative to positive rapidity than in Ref.[2], while for the “ $\gamma +jet$ ” final state our results are higher by 25% to 10%, respectively.

4 Conclusion

Results of the NLO calculation for the isolated γ production in DIC process at HERA are presented. In addition

two NNLO contributions: double resolved photon processes and box diagram were studied. The satisfactory agreement with data is obtained for both “ γ ” and “ $\gamma+jet$ ” events for the rapidity distribution. The box diagram contributes 13% to the “direct” sample as measured by ZEUS group.

The agreement with the other NLO calculation of the DIC, which based on a different set of diagrams, is obtained within 10 to 25%.

Acknowledgements

We thanks P. Bussey and L. Gordon for important discussions. MK is grateful to Stan Brodsky for useful discussions and hospitality during her stay at SLAC.

Supported by Grant No 2P03B18410.

References

1. M. Krawczyk, unpublished; J. Żochowski, MS thesis 1992; M. Krawczyk, A. Zembruski, J. Żochowski - in preparation
2. L.E. Gordon, *Phys. Rev. D* **57**, 235 (1998)
3. ZEUS Coll., DESY-97-146 (hep-ex/9708038); submitted to ICHEP’98, Vancouver, 1998
4. J.D. Bjorken, E.A. Paschos, *Phys. Rev.* **185**, 1775 (1969)
5. T.Tu, C. Wu, *Nucl. Phys. B* **156**, 493 (1979)
6. D.W.Duke, J.F. Owens, *Phys. Rev. D* **26**, 1600 (1982); P. Aurenche *et al.*, *Z. Phys. C* **24**, 309 (1984), *Z. Phys. C* **56**, 589 (1992)
7. M. Krawczyk, *Acta Physica Pol.* **21**, 999 (1990); A.C.Bawa, M. Krawczyk and W.J.Stirling, *Z. Phys. C* **50**, 293 (1991); A.C. Bawa and M. Krawczyk, Proc. “Physics at HERA”, Hamburg 1991, p. 579, and IFT 91/17; B.L. Combridge, *Nucl. Phys. B* **156**, 493 (1979) M. Fontannaz, D. Schiff, *Z. Phys. C* **14**, 151 (1982)
8. L.E. Gordon, W. Vogelsang *Phys. Rev. D* **52**, 58 (1995)
9. A. Zembruski, IFT 10/98, and PhD thesis in preparation
10. M. Glück, E. Reya and A. Vogt, *Z. Phys. C* **67**, 433 (1995); *Phys. Rev. D* **46**, 1973 (1992); *Phys. Rev. D* **48**, 116 (1993)
11. P. Aurenche *et al.*, *Z. Phys. C* **56**, 589 (1992)
12. L.E. Gordon, J.K. Storrow, *Z. Phys. C* **56**, 307 (1992)
13. in preparation